HYDROXYAPATITE COATINGS ON Cp-TITANIUM GRADE-2 SURFACES PREPARED WITH PLASMA SPRAYING

NANOS HIDROKSIAPATITA NA POVRŠINO Cp-TITANA GRADE-2 Z NABRIZGAVANJEM S PLAZMO

Rebeka Rudolf[1], Dragoslav Stamenković[2], Zoran Aleksić[2], Monika Jenko[3], Igor Đorđević[2], Aleksandar Todorović[2], Vukoman Jokanović[4], Karlo T. Raić[5]

[1]University of Maribor, Faculty of Mechanical Engineering, Maribor, Slovenia
[2]University of Belgrade, School of Dental Medicine, Belgrade, Serbia
[3]Institute of Metals and Technology, Ljubljana, Slovenia
[4]University of Belgrade, VINCA Institute of Nuclear Sciences, Belgrade, Serbia
[5]University of Belgrade, Faculty of Technology and Metallurgy, Belgrade, Serbia
karlo@tmf.bg.ac.rs

Thin hydroxyapatite coatings were produced on Cp-Titanium Grade-2 samples, with new high-voltage pulse-power equipment PJ-100 (Plasma Jet, Serbia) in order to get a more stable implant structure appropriate for further clinical applications. A comparative analysis of differently prepared surfaces of the Cp-Titanium Grade-2 samples was done before the hydroxyapatite was applied.
Microstructural observation of the modified hydroxyapatite/implant surface was done using scanning-electron-microscopy imaging and Auger electron spectroscopy, with the aim of detecting the morphology and the elements contained in the new surfaces of the samples. The results confirmed that the surface of Cp-Titanium Grade-2 modified with hydroxyapatite is very similar to the bone structure.

Keywords: Cp-Ti2 material, hydroxyapatite (HA), plasma-spray coating, characterization

Z novo, visokonapetostno pulzirajočo plazemsko napravo PJ-100 (plasma Jet, Serbia) je bil pripravljen tanek nanos hidroksiapatita na vzorce iz Cp-Titan Grade-2, da bi dobili bolj stabilno strukturo vsadka za klinično uporabo. Izvršena je bila primerjalna analiza različno pripravljenih površin vzorcev iz Cp-Titana Grade-2, preden je bil izvršen nanos hidroksiapatita.
Opazovanje mikrostrukture s hidroksiapatitom modificirane površine vsadka je bilo izvršeno z vrstično elektronsko mikroskopijo, kot tudi z Augerjevo elektronsko spektroskopijo, z namenom odkritja morfologije in razporeditve elementov na novi površini vzorca. Rezultati so potrdili, da je modificirana površina Cp-Titana Grade-2 s hidroksiapatitom zelo podobna strukturi kosti.

Ključne besede: material Cp-Ti2, hidroksiapatit (HA), s plazmo nabrizgan nanos, karakterizacija

1 INTRODUCTION

Titanium (Ti) has two most useful metal properties: corrosion resistance and the highest strength-to-weight ratio compared to other metals. Moreover, when in the unalloyed condition, it is stronger than some other similar materials, such as contemporary steel, and it is more than 40 % lighter. Ti can be alloyed with various elements (Al, V, Nb, Zr) that can additionally improve its strength, while maintaining high temperature performance, creep resistance, weldability, response to ageing heat treatments and formability. Ti and its alloys are resistant to corrosion because of the formation of an insoluble and continuous titanium-oxide layer on the surface having one of the highest heats of reaction: $\Delta H = -912$ kJ/mol. In air, an oxide (usually TiO_2) begins to form within nanoseconds (10^{-9} s) and reaches a thickness of 2–10 nm already in 1 s. This oxide is very adherent to the parent Ti, protecting the metal from other impurities and it is impenetrable to oxygen[1]. Moreover, this oxide on the Ti-surface gives Ti its excellent biocompatibility[2]. Commercially pure (Cp) Ti is available in four grades (1–4) that vary with respect to oxygen ($w = 0.18$–0.40 %)

and iron ($w = 0.20$–0.50 %) amounts. These slight concentration differences have a substantial effect on the physical properties of the metal. Oxygen, in particular, has a great influence on the ductility and strength of Ti[3]. In our investigation we used Cp-Titanium Grade-2 (Cp-Ti2) materials which have the medium value of O. Cp-Ti2 is used widely because it combines excellent formability and moderate strength with superior corrosion resistance. This combination of properties makes Cp-Ti2 a good candidate for medical applications, i.e., implant manufacturing.

These materials are classified as biologically inert biomaterials. This means that they remain essentially unchanged when implanted into human bodies[4–6]. The human body is able to recognise these materials as foreign and tries to isolate them by encasing them in fibrous tissues. However, they do not cause any adverse reactions and are tolerated well by the human tissues[7]. Although the bulk properties of biomaterials are important with respect to their biointegration, the biological responses of the surrounding tissues to dental implants are controlled mostly with their surface characteristics

(chemistry and structure) because biorecognition takes place at the interface of an implant and the host tissue. Biological tissues mainly interact with the outermost atomic layers of an implant, which are about 0.1–1 nm thick. The molecular and cellular events at the bone-implant interface are well described[8], but many crucial aspects are still far from being understood. A justification of the surface modification of implants is, therefore, straightforward: to retain the key physical properties of an implant while modifying only the outermost surface to control the bio-interaction. As a result, a lot of research work is devoted to elaborate methods of modifying the surfaces of the existing implants (biomaterials) to achieve the desired biological responses.

With respect to the presented problems of the state-of-the-art implant surface, the main question of our research was how to prepare the ideal micro-topography of the selected Cp-Ti2 material. In this framework we took into consideration that the most common physico-chemical treatments are chemical surface reactions (e.g., oxidation, acid-etching), sand blasting, ion implantation, laser ablation, coating the surface with inorganic hydroxyapatite, etc. These methods alter the energy, charge and composition of the existing surface, but they can also provide the surfaces with modified roughness and morphology[9].

Although more accurate knowledge is required, typical Cp-Ti2 surfaces were treated with different high-voltage-plasma process parameters. In this manner we wanted to test the experimental presentation of the thin hydroxyapatite (HA) coating on the Cp-Ti2 samples using a specific plasma installation[10]. The aim of this work was, namely, to produce a thin HA coating with the new methods in order to get a more stable surface structure of Cp-Ti2 that could be used for further clinical applications. Finally, a comparative analysis was done using the classical preparation method, chemical etching, in order to acquire the information about the new plasma technology.

2 MATERIALS AND METHODS

The samples for the experiments were made from the Cp-Ti2 material (ASTM F 67-100) with a chemical composition in mass fractions as follows: $w(C)_{max} = 0.08$ %, $w(N)_{max} = 0.030$ %, $w(O)_{max} = 0.25$ %, $w(Fe)_{max} = 0.30$ %, $w(H) = 0.015$ %. The properties of Cp-Ti2 are: the melting point of 1668 °C, a Vickers hardness of 180 HV, a 0.2 % yield strength of 275–450 MPa, a tensile strength of > 350 MPa, an elongation of > 20 %, a density of 4.5 g/cm³, the coefficient of thermal expansion of 25–400 °C 9.4×10^{-6}/K, and elasticity modulus of 110 GPa. The samples were produced in the shape of discs with the dimension of $\phi = 10$ mm and a thickness of 2 mm.

It is well known that the adhesion between a ceramic coating (HA) and a metal implant is strongly influenced

by the metal surface roughness. Therefore, the process of roughening is adjusted to the optimum level with several parameters: pressure of water, air flow, corundum granulation and diameter of the nozzle for roughening. The chamber for roughening was constructed in-house from hardened steel. The tool for capturing the samples (also our own construction) was used as a separate set of tools, rotating at more than 1000 r/min. The roughening of the samples was done under the following conditions: a fluid pressure of 8 bar, a nozzle diameter of $\approx$ 10 mm and a corundum granulation of 1–2 mm. The obtained surface roughness (R_a) was in the range from 4.72 μm to 5.28 μm (a Perthen Perthometer). After the roughening, the samples were washed with toluene and acetone to remove the traces of oil from the compressor. The specimens were then immersed in 5.0 mL of 5 M NaOH aqueous solution for 24 h. Afterwards they were removed from the solution and washed gently with distilled water, followed by drying at 40 °C for 24 h in an air atmosphere. The treated metal was then heated up to 300 °C (Sample F_1), 500 °C (Sample F_2), 700 °C (Sample F_3) and 800 °C (Sample F_4) at a rate of 5 °C/min in an Ni–Cr electrical furnace in an air atmosphere over 5 h. After the thermal treatment all the samples were cooled to room temperature in the furnace. An untreated sample (Sample F_0) was used for obtaining a better insight into the differences between the treated and untreated samples.

The plasma installation PJ-100 (Plasma Jet, Serbia) was used for the plasma-spray process[10,11]. The basic parameters of the installation used for applying HA depositions were: a power of (52.0 ±1.5) kW, a voltage of (120±2) V, a current of (430±5) A, an argon flow of (38.5±1.2) L/min, powder carrier gas, air of 8 L/min and a powder-mass input of (2.0±0.1) g/s. The samples were placed on a drum ($\phi = 200$ mm) of the plasma installation (a rotation velocity of 3.7 r/s) for the HA deposition. The complete coating process was performed in 2–3 short intervals taking 7 s to 10 s each, with a break rate of a few minutes between the cycles of deposition. Before the plasma treatment Ti disks were heated at a temperature of 200 °C, which was found to be the optimum for obtaining the maximum partition of the HA crystalline phase in the process of its deposition. Two commercially available HA powders were used: HA powder XPT-D-703 (Sulzer Metco, USA) and HA powder Captal 90 (Plasma Biotal, UK). The granulations of the powders were obtained from the manufacturers' specifications.

A microstructural characterization of the samples was carried out with scanning electron microscopy (SEM-Sirion 400 NC), in addition to an energy-dispersive X-ray (EDX) analysis (Oxford INCA 350). The specimens were observed directly without any surface preparation.

Detailed microstructure observations of the obtained surfaces were done using field-emission Auger electron spectroscopy (FE-AES) – a Thermo Scientific Microlab

310-F spectrometer equipped with a spherical-sector analyser and a field-emission electron gun with a thermally assisted Schottky field-emission source providing a stable electron beam in an accelerating voltage range of (0.5–25) keV.

3 RESULTS AND DISCUSSION

3.1 Microstructure observation of Cp-Ti2 surfaces

Typical microstructures of the Cp-Ti2 surfaces after different processes of roughening are shown in **Figure 1**.

From the pictures it can be concluded that immersion in NaOH represents a technique which results in obtaining a high surface roughness (**Figure 1a**). On the other hand, the thermal treatment at different temperatures represents the attainable method for surface roughness. At lower temperatures the roughness is lower (**Figures 1b, 1c, 1d**) and, consequently, at higher temperatures the roughness is higher (**Figure 1e**).

This is very important for the quality of the HA coating textures on dental Cp-Ti2 implants. The ideal microtopography of a Cp-Ti surface is still unknown because it is very difficult to associate Cp-Ti/HA interface properties with clinical results[12].
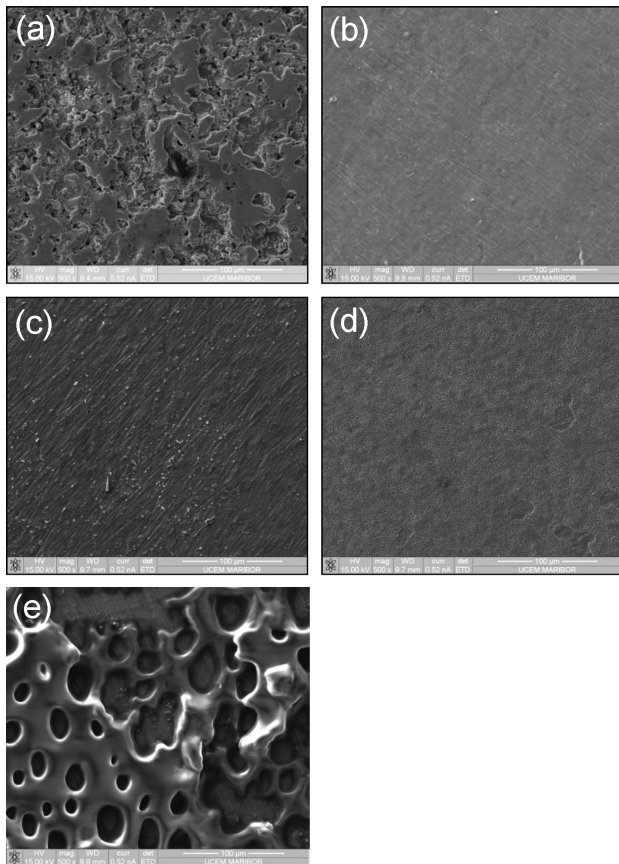
3.2 Microstructure observation of HA/Cp-Ti2 surfaces

Using FE-AES spectroscopy we discovered that the cross-sections of the HA coatings for samples F_0-F_4 obtained with plasma-jet deposition clearly show their depths, as shown in **Table 1**.

Table 1: HA coating depth
Tabela 1: Debelina HA-nanosa

Sample label	Average depth, nm	Maximum depth, nm	Minimum depth, nm	Maximum deviation from the average value, nm
F_0	206	221.7	192.9	15.7
F_1	205.8	216.2	191.4	14.4
F_2	152.4	172.2	138.5	19.8
F_3	156.2	167.4	140.7	15.4
F_4	156.1	164.3	146.5	9.7

According to the data given in **Table 1** there are no significant differences in the depth of these coatings. For the same sample (the same conditions of their plasma treatment) the variety of the depths along the entire section was in the range of ± 20 nm. These values show a very uniform depth of the coating for each sample, with the maximum depth deviation (from its average value) between (9.7 and 19.8) nm.
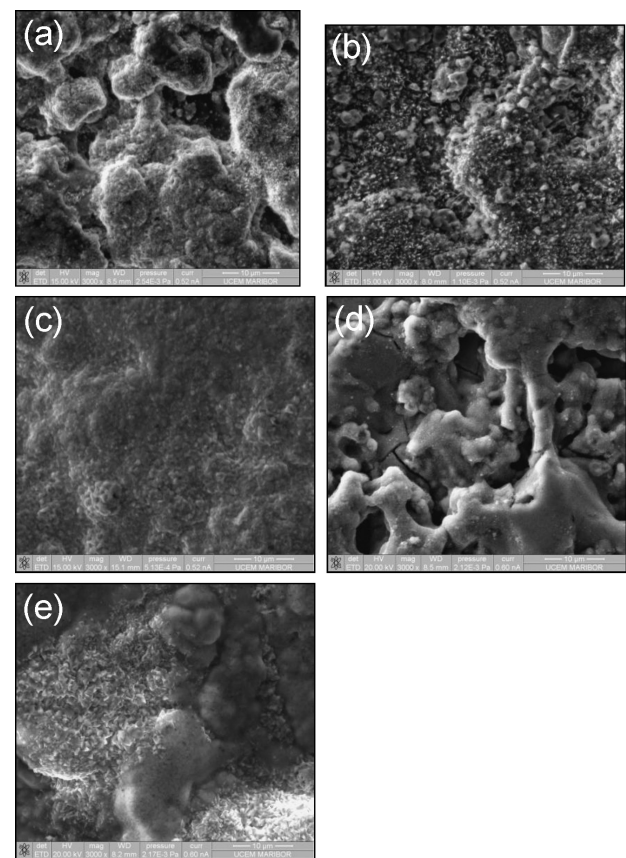

Figure 1: SEM micrographs of Cp-Ti2 surfaces: a) F_0, b) F_1, c) F_2, d) F_3 and e) F_4
Slika 1: SEM-posnetki površine Cp-Ti2: a) F_0, b) F_1, c) F_2, d) F_3 in e) F_4

Figure 2: SEM micrographs of HA coating on different substrates: a) F_0, b) F_1, c) F_2, d) F_3 and e) F_4
Slika 2: SEM-posnetki HA nanosa na različnih podlagah: a) F_0, b) F_1, c) F_2, d) F_3 in e) F_4

The HA coating of sample F_0 (**Figure 2a**) shows a typical, very rough surface, with a very interesting morphology. The smallest sizes of the mosaic details were only a few µm, while very large and mutually interconnected parts were dominant. The obtained form is typical for quickly cooled systems that were exposed to melting at the edges of various particles. The specific form of the surface topology seems to be very promising for the cell adhesion. The structure is layered showing strongly exposed hills and valleys. In some places very deep voids can be observed. The mosaic details with an irregular form of very large agglomerates show the dimensions of about 50 µm.

The HA coating of sample F_1 (**Figure 2b**) shows a fairly homogenous surface with almost parallel patterns that look like textile fibres. The motifs are more discreet. The intertwined details are very ordered, with slightly raised or lowered parts. The details have the size of about 1 µm or less.

The HA coating of sample F_2 (**Figure 2c**) has a very rough surface with almost parallel patterns and it is sprinkled with white and black motifs resembling furrows, with the corresponding typical morphology. Very light details show individual particle sizes between (0.7 and 2.9) µm.

The HA coating of sample F_3 (**Figure 2d**) shows a specific surface morphology with a worm-like structure and finer, more expressed grains than in the previous cases. Individual particles are clearly visible. Their values are between 0.3 µm and 0.6 µm. The mosaic is very uniform. The grains are elongated and of a prismatic form. There are no visible voids and it seems that the layers of HA were sorted properly, without a build-up causing the creation of valleys and hills, as shown for samples F_0-F_2.

The HA coating of sample F_4 (**Figure 2e**) shows a very specific layout of cavities and elevations. It looks like a very nicely knitted network with several visible layers and holes with the dimensions of 7–36 µm. The depths of the continuous, interconnected parts of the network are of fairly similar dimensions. These morphologies show the first layer below the perforated layers (the ropes in network) with a fairly flat surface and small parallel patterns. The sizes of individual particles are between 0.25 µm and 1.45 µm.

The EDS analysis of the HA coating (**Figure 3**) shows all the elements present inside the coating from the titanium substrate to the top of the coating. The part of the substrate changed during the plasma-jet deposition can be also seen on the corresponding picture.

The concentrations of various elements given in the above diagrams show very similar data: the boundaries between the Ti substrate and HA coatings are clearly visible. In all the cases, small quantities of oxygen and aluminum are noticed, while the concentration of Ti deceases strongly, reaching a zero value. On the left side
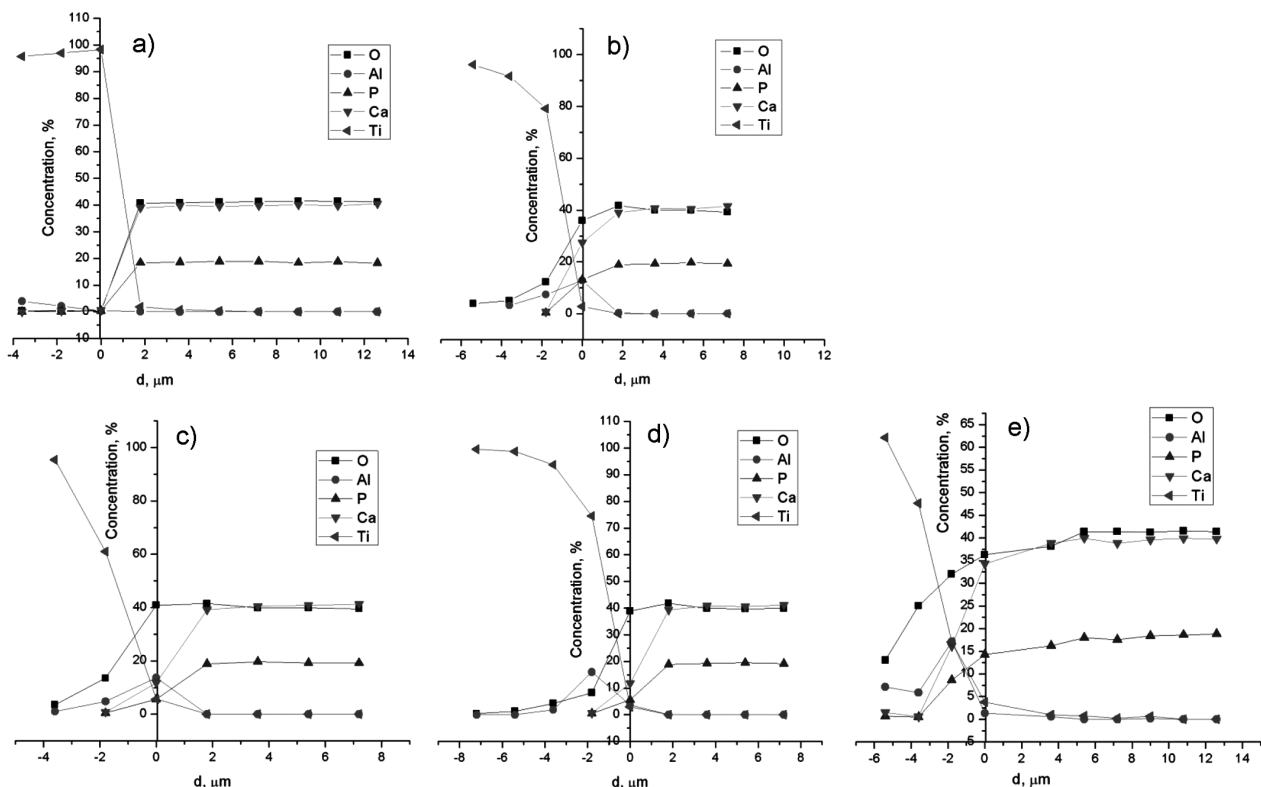

Figure 3: EDS analysis of the cross-sections of various samples of HA coatings: a) F_0, b) F_1, c) F_2, d) F_3 and e) F_4 depending on the distance from the left or right side of the boundary

Slika 3: EDS-analiza prereza različnih vzorcev HA-nanosa: a) F_0, b) F_1, c) F_2, d) F_3 in e) F_4, v odvisnosti od razdalje od meje levo ali desno

of the boundary, small quantities of calcium and phosphorous were registered. Also, in this area, at a distance of 3.6 μm, the highest level of Al was noticed for sample F_0 ($w = 3.95$ %), while for F_1, F_2, F_3 and F_4 the highest levels of Al were noticed at the following boundaries: $w = 12.8$ % for F_1, $w = 13.7$ % for F_2, $w = 16$ % for F_3 and $w = 17$ % for F_4. The oxygen level was very low on the left side of the boundary for the untreated sample F_0, while for sample F_1 it was between $w = 3.9$ % at a distance of 3.6 μm left of the substrate boundary and $w = 35$ % at the boundary; for sample F_2 it was $w = 1.1$ % at a distance of 3.6 μm left of the boundary and $w = 13.7$ % at the boundary; for sample F_3 it was $w = 1.9$ % at a distance of 1.8 μm left of the boundary and $w = 16$ % at the boundary; and for F_4 it was $w = 20.45$ % at a distance of 3.6 μm left of the boundary and $w = 41.5$ % at the boundary. The boundary was narrower or wider, and the mixing of ions from the right and left sides of the boundary was clearly visible at a distance of 1.8 μm left of the boundary (for samples F_2, F_3 and F_0). For samples F_1 and F_4 the

boundary was narrower and the decrease in Ti was very sharp. The maximum depth of penetration of Ca and P ions in all the cases was about 3.8 μm inside the substrate depth. These values show good agreement for all the samples. Inside the HA coatings, at a distance of 1.8 μm on the right, there was no more interference, i.e., the mixing of the ions from the Ti substrate with the ions contained inside the HA coating. In deeper layers of HA coatings the concentrations of Ca, P and O ions reached
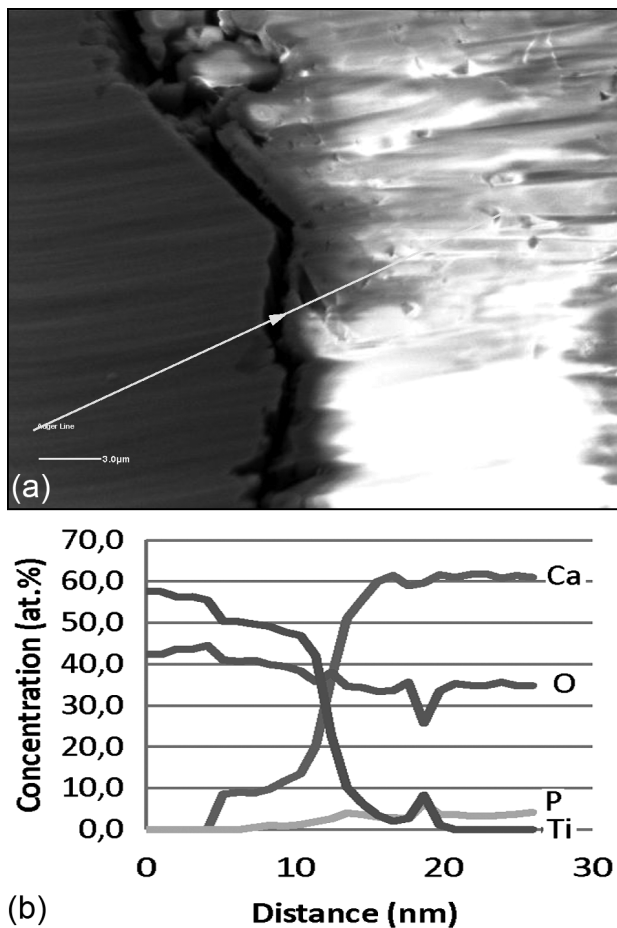

Figure 4: a) SEM image of the interface, line-scanned with AES, between the substrate and HA layer for sample F_1, b) AES line scan of the interface between HA and the substrate indicating the concentrations of Ca, O, Ti and P
Slika 4: a) SEM-posnetek stika, kjer je bila izvršena AES linijska analiza med podlago in HA-nanosom pri vzorcu F_1, b) AES linijska analiza stika HA in podlage, ki prikazuje koncentracijo elementov Ca, O, Ti in P
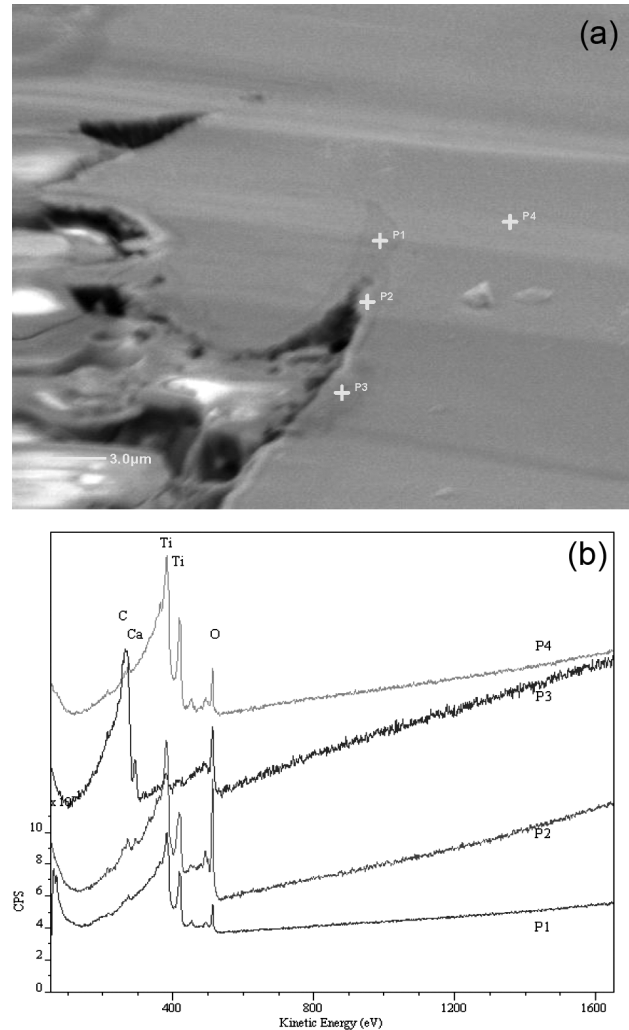

Figure 5: a) SEM image with marked places of AES, b) AE spectra for the spots in a)
Slika 5: a) SEM-posnetek točk AES-analize, b) AES-spektri v točkah iz a)

Table 2: Measured elements using AES, amount-of-substance, x/%
Tabela 2: Merjenje elementov z AES, množinski delež, x/%

Spot	Concentration, x/%			
	C	Ca	O	Ti
P1	11.2	0.0	35.2	53.6
P2	12.2	6.5	60.4	20.9
P3	46.3	25.6	24.3	3.8
P4	17.6	3.6	31.0	47.8

saturation, becoming uniform with a further increase in the distance.

A typical secondary electron image (SEI) of the interface, line-scanned with Auger electron spectroscopy (AES), between the substrate and HA coatings for sample F_1, and a spectrogram of the distributions of Ca, O, Ti and P are given in **Figure 4**.

This figure clearly shows a decrease in the Ti amount (present until the depth of the coating reaches a value of 20 nm) and an increase in the Ca in the coating between 4 nm and 17.5 nm. Both of these curves are typical S curves, inversely relative to one another. The oxygen amount decreases slightly, showing its highest value inside the chemically and thermally treated part of titanium (between 0 nm and 4 nm). In the area of the HA coating its amount reduces slightly by 4 nm and 10 nm (the part in which Ca atoms are propagated due to a high velocity of the calcium-hydroxide particles melted on the surfaces by the plasma jet). Afterwards, the oxygen amount varies statistically within certain limits.

Similar results are shown in **Figure 5**, where the concentrations of various elements, measured in counts per second (CPS), are explained with respect to the kinetic energy of the back-scattering electrons. Particular values of these energies prove the presence of Ca, Ti and O, showing their changes between sites P_1–P_4 (the sites at various distances from the boundary with hydroxyapatite). Besides, these values are given in **Table 2** for each of the observed sites.

Finally, as reported by Kokubo[13] and Kim[14], the calcium-phosphate deposition obeys the nucleation process. The electric-charge interaction also heavily favours this process. A higher surface energy favours the calcium phosphate initiating nucleation and the basic TiOH with the negative charge can adsorb the positively charged calcium ion (Ca^{2+}) first adsorbed to neutralize the surface charge until too much charge accumulates producing a positive layer of calcium titanate. Then, this positive layer interacts further with the negatively charged phosphate ion (PO_4^{3-}) to form the amorphous calcium phosphate, which will be crystallized further into an OCP phase despite the fraction of the amorphous calcium-phosphate residue.

4 CONCLUSIONS

The innovative plasma-jet process of hydroxyapatite deposition with a previous preparation of titanium substrates with NaOH etching and a subsequent thermal treatment is shown in this paper. In addition, the as-deposited coatings were composed mainly of the HA phase with the crystallite sizes between 15.5 nm and 31 nm.

Furthermore, Auger electron spectroscopy, through Ca-ion implantation in the depth of the oxide area of the substrate, shows the processing advantages that, consequently, led to the increased adhesion strength. Therefore, this improved plasma-jet method, with an unusually high kinetic energy of the plasma, seems to be promising for the fabrication of nanostructured HA coatings with unique microstructural features, which are desirable for enhancing the biological properties of HA coatings.

Research confirms a high potential of a deposition of HA on titanium substrates via a new plasma installation for any medical purpose.

Acknowledgements

5 REFERENCES

[1] E. P. Lautenschlager, P. Monaghan, Titanium and titanium alloys as dental materials, Int Dent J, 43 (**1993**) 3, 245–53

[2] B. D. Ratner, A. S. Hoffman, F. J. Schoen, J. E. Lemons, Biomaterials science: an introduction to materials in medicine, Academic Press, New York 1996

[3] H. M. Kim et al., Thin film of low-crystalline calcium phosphate apatite formed at low temperature, Biomaterials, 21 (**2000**), 1129–1134

[4] L. Le Guehennec, A. Soueidan, P. Layrolle, Y. Amouriq, Surface treatments of titanium dental implants for rapid osseointegration, Dental Materials, 23 (**2007**), 844–854

[5] G. Daculsi, O. Laboux, O. Malard, P. Weiss, Current state of the art of biphasic calcium phosphate bioceramics, Journal of Materials Science: Materials in Medicine, 14 (**2003**), 195–200

[6] Z. T. Sul et al., The bone response of oxidized bioactive and non-bioactive titanium implants, Biomaterials, 24 (**2003**), 3893–3907

[7] K. Turzo, Surface Aspects of Titanium Dental Implants, In: R. H. Sammour (ed.), Biotechnology – Molecular Studies and Novel Applications for Improved Quality of Human Life, InTech, Rijeka 2012, 237 (www.intechopen.com)

[8] D. A. Puleo, A. Nanci, Understanding and controlling the bone-implant interface, Biomaterials, 20 (**1999**), 2311–2321

[9] B. Kasemo, Biological surface science, Surface Science, 500 (**2002**), 656–677

[10] M. Vilotijević, Dc plasma arc generator with increasing volt-ampere characteristic, RS Patent No 49, 7062007, 2007

[11] J. Ružic et al., Understanding plasma spraying process and characteristics of DC-arc plasma gun (PJ-100), Metallurgical & Materials Engineering, 18 (**2012**), 273–282

[12] I. Milinković et al., Aspects of titanium-implant surface modification at the micro and nano levels, Mater. Tehnol., 46 (**2012**) 3, 251–256

[13] T. Kokubo, H. M. Kim, M. Kawashita, Novel bioactive materials with different mechanical properties, Biomaterials, 24 (**2003**) 13, 2161–2175

[14] H. M. Kim et al., Surface potential change in bioactive titanium metal during the process of apatite formation in simulated body fluid, Journal of Biomedical Materials Research, Part A, 67A (**2003**) 4, 1305–1309